Electronic Supplementary Material (ESI) for Chemical Science.

Supplementary Information

Switching between classical/nonclassical crystallization pathways of TS-1 zeolite: implication on titanium distribution and catalysis

Risheng Bai,[a, b] Yue Song,[a] Lukas Lätsch,[c] Yongcun Zou,[a] Zhaochi Feng,[d] Christophe Copéret,[c] Avelino Corma,*[b] and Jihong Yu*[a, e]

a State Key Laboratory of Inorganic Synthesis and Preparative Chemistry, College of Chemistry, Jilin University Changchun 130012, China

b Instituto de Tecnología Química, Universitat Politècnica de València-Consejo Superior de Investigaciones Científicas, Valencia 46022, España

c ETH Zürich – H229, Department of Chemistry and Applied Biosciences, CH-8093 Zürich

d State Key Laboratory of Catalysis, Dalian Institute of Chemical Physics, Chinese Academy of Sciences, Dalian 116023, China

e International Center of Future Science, Jilin University, Changchun 130012, China

Correspondences: acorma@itq.upv.es (A.C.) and jihong@jlu.edu.cn (J.Y.)

Table of Contents

Experimental section

Reactant agents. All reagents were used as purchased commercially without any further purification. Tetrapropylammonium hydroxide (TPAOH) (40 wt%, Adamas). Tetraethyl titanate (TEOT, 98%), tetrabutyl titanate (TBOT, ≥99%), and tetra-2-ethylhexyl titanate (TEHOT, 98%) were purchased from Aladdin Co. Tetraethyl orthosilicate (TEOS, ≥99%), dimethoxydimethylsilane (99.5%), triethylamine (99%), 4,6-dimethyldibenzothiophene (4,6-DMDBT, 97%), tert-butyl hydroperoxide solution (70 wt%), 1-hexene (>99%), 2-methyl-2-butene (≥95%), cyclohexene (99%), and hydrogen peroxide solution (H_2O_2, 35 wt%) were purchased from Sigma-Aldrich.

Preparation of silicalite-1 (S-1) and titanosilicate TS-1 zeolites. The S-1 and titanosilicate TS-1 zeolites were prepared with the following molar composition: 1.0 SiO_2: (0-0.035 TiO_2): 0.2 TPAOH: 10–40 H_2O under static hydrothermal conditions (170 °C), with tetrapropylammonium hydroxide (TPAOH) as the organic structure directing agent and with tetraethyl titanate (TEOT), tetrabutyl titanate (TBOT), or tetra-2-ethylhexyl titanate (TEHOT) as the Ti source. Typical synthesis procedure is as follows: mixing 2.540 g TPAOH (40 wt%) with 3.876 g distilled water and stir for 15 min; afterward, add 0.213 g TBOT and 5.208 g tetraethyl orthosilicate (TEOS) into the system and stir for 8 h to get the complete hydrolysis. Then introduce the synthesis gel into a Teflon-lined stainless-steel autoclave. Crystallization is carried out at 170 °C under static conditions for different crystallization times. After centrifugation, washing, and drying with water and ethanol, the products were calcined at 550 °C for 6 h under air atmosphere to remove the organic template.

Preparation of TS-1-NC and TS-1-C zeolites. Titanosilicate zeolites (TS-1-NC and TS-1-C) were prepared with the following molar composition: 1.0 SiO_2: 0.025 TiO_2: 0.2 TPAOH: 10–40 H_2O under static hydrothermal conditions (170 °C), with TPAOH as the organic structure directing agent and with TBOT as the Ti source. Typical synthesis procedure is as follows: mixing 2.540 g TPAOH (40 wt%) with 3.876 g distilled water and stir for 15 min; afterward, add 0.213 g TBOT and 5.208 g TEOS into the system and stir for 8 h to get the complete hydrolysis. Then introduce the synthesis gel into a Teflon-lined stainless-steel autoclave. Crystallization is carried out at 170 °C under static conditions for 12 h. After centrifugation, washing, and drying with water and

ethanol, the products were calcined at 550 °C for 6 h under air atmosphere to remove the organic template.

Preparation of the amorphous titanosilicate precursor seeds. Titanosilicate precursor seeds（TS-1-NC-Amorphous Seed and TS-1-C-Amorphous Seed) were prepared with the following molar composition: 1.0 SiO_2: 0.025 TiO_2: 0.2 TPAOH: 10–40 H_2O (10 H_2O for the TS-1-NC-Amorphous Seed and 40 H_2O for TS-1-C-Amorphous Seed) under static hydrothermal conditions (170 °C), with TPAOH as the organic structure directing agent and with TBOT as the Ti source. Typical synthesis procedure is as follows: mixing 2.540 g TPAOH (40 wt%) with 3.876 g distilled water and stir for 15 min; afterward, add 0.213 g TBOT and 5.208 g TEOS into the system and stir for 8 h to get the complete hydrolysis. Then introduce the synthesis gel into a Teflon-lined stainless-steel autoclave. Crystallization is carried out at 170 °C under static conditions for 1 h.

Preparation of TS-1-NC-S and TS-1-C-S zeolites. Typical synthesis procedure for the preparation of Titanosilicate zeolites (TS-1-NC-S and TS-1-C-S) is as follows: mixing 2.540 g TPAOH (40 wt%) with 17.376 g distilled water and stir for 15 min; afterward, add 5.208 g TEOS into the system and stir for 8 h to get the complete hydrolysis; then add 400 mg of the amorphous titanosilicate precursor seeds（TS-1-NC-Amorphous Seed or TS-1-C-Amorphous Seed) and stir for 10 min. Then introduce the synthesis gel into a Teflon-lined stainless-steel autoclave. Crystallization is carried out at 170 °C under static conditions for 24 h. After centrifugation, washing, and drying with water and ethanol, the products were calcined at 550 °C for 6 h under air atmosphere to remove the organic template.

Silylation conditions. The silylation process was performed using a standard procedure under N_2 flow. Calcined TS-1-TBOT-10 or TS-1-TBOT-40 zeolite (1 g) previously dehydrated at 300 °C under vacuum was contacted with a solution of silylating agent (dimethoxydimethylsilane, 0.338 g) in dry toluene (10 mL) at 80 °C under reflux for 1 hour. Then, a solution of triethylamine (0.338 g) in toluene (5 mL) was also added and the mixture was refluxed for an additional hour at 80 °C. The zeolite was washed with toluene and dried at 100 °C. The silylated TS-1-TBOT-10 and TS-1-TBOT-40 samples were named as TS-1-TBOT-10-sil and TS-1-TBOT-40-sil, respectively.

Characterizations

Powder X-ray diffraction analysis of the samples was carried out on a Rigaku D-Max 2550 diffractometer using Cu Kα radiation (λ = 1.5418 Å, 50 KV).

Transmission electron microscopy (TEM) images were recorded on JEM-2100F and Tecnai F20 electron microscope.

Scanning electron microscopy (SEM) images were recorded on JSM-6700F (JEOL) electron microscope.

Nitrogen adsorption-desorption measurements were carried out on a Micromeritics ASAP 3-flex analyzer at 77 K. Before starting the N_2 adsorption measurements, all the samples were activated by degassing in-situ at about 573 K for 10 h.

Chemical compositions were determined with Inductively Coupled Plasma-Optical Emission Spectrometry (ICP-OES) analysis performed on an iCAP 7000 SERIES.

The particle size was measured by photon correlation spectroscopy employing a Nano ZS90 laser particle analyzer (Malvern Instruments, UK) at 25 °C.

Atomic Force Microscope (AFM) images were recorded in the tapping mode with a Nanoscope IIIa scanning probe microscope from Digital Instruments under ambient conditions.

The Ultraviolet Visible diffuse reflectance spectroscopy (UV-Vis DRS) of the catalysts was recorded over the range of 190 nm to 500 nm against the support as reference, on a SHIMADZU U-4100.

Infrared spectra with adsorption-desorption of pyridine were carried out on self-supported wafers (10 $mg \cdot cm^{-2}$) activated at 673 K and 10^{-2} Pa for 12 h. After sample activation, pyridine vapor (6.5×10^2 Pa) was admitted into the vacuum IR cell and adsorbed onto the zeolite at room temperature. Desorption was performed under vacuum over two consecutives 1 h periods of heating at 323 K and 373 K, each followed by a Nicolet 710 FT-IR spectrometer measurement at room temperature. All spectra were scaled according to the sample weight.

Ultraviolet Raman resonance spectroscopy (UV-Raman) were recorded on a DL-2 Raman spectrometer using the 266 or 320 nm line of a He-Ge laser as the excitation source and a Princeton CCD as the detector.

All the ^{17}O solid-state NMR measurements were obtained on a Bruker Avance III 600-MHz NMR spectrometer (14.1 T) at low temperatures (100 K) using a 3.2-mm probe. The magnetic field was externally referenced by setting the signal of liquid H_2O (at room temperature) to 0 ppm. Measurements were performed in a 3.2-mm sapphire rotor closed with a zirconia cap. Static WURST-CPMG (wideband, uniform-rate and smooth-truncation pulse with CPMG echo-train acquisition) experiments were performed to obtain the ^{17}O NMR spectra. Details of the WURST pulse are as follows: length, 50 μs; 80 steps; sweep width, 0.5 MHz, sweeping from low to high frequency. The recycle delay was set to 0.7 s. SPINAL64 with 100-kHz radio frequency was used for ^{1}H decoupling. The parameters obtained from fitting the individual signals for the μ_2-peroxo are: δ_{iso} = 420 ppm, $\Delta\delta$ = 101 ppm, η_{CST} = 0.58, C_Q = 16.5 MHz, η_{EFG} = 0.24, LB = 37 ppm, φ = 90°, X = 0° , Ψ = 0° and for H_2O: δ_{iso} = 30 ppm, C_Q = 6.1 MHz, η_{EFG} = 0.1, LB = 4 ppm.

Catalytic tests

Oxidative desulfurization of 4,6-dibenzothiophene (4,6-DMDBT). A model fuel with a sulfur concentration of about 500 ppm was prepared by dissolving 4,6-DMDBT in n-dodecane. The oxidative desulfurization reaction was performed in a 50 mL three-necked round-bottom flask, connected to a reflux cooler system with magnetic stirring. The catalyst was activated at 473 K for 2 h before used. Typically, 30 mg catalyst was added into 7 g of model fuel, then 25 mg n-octadecane and 28.2 mg of TBHP were added in turn, which acted as internal standard and oxidant, respectively. The reaction was carried at 343 K for 15 min under magnetic stirring of 1400 rpm to eliminate the effects of the external mass transfer resistances of the catalysts. The products were analyzed by Gas Chromatography-Mass Spectrometry (GC-MS, Thermo Fisher Trace ISQ, equipped with TG-5MS column, L=60 m). Mass balances were accurate to within 5%.

Epoxidation of alkenes (1-hexene, 2-methyl-2-butene, and cyclohexene). The epoxidation of alkenes (1-hexene, 2-methyl-2-butene, or cyclohexene) with H_2O_2 as oxidant, undecane as internal standard, and methanol or acetonitrile as the solvent was carried out in batch reactors. The catalyst was activated at 473 K for 2 h before used. In a typical run, 1-hexene (16 mmol), H_2O_2 (4 mmol), catalyst (100 mg), and methanol (12 g) were added into the batch reactor and pressurized the reactor to 3 bars of nitrogen. The reaction was carried at 323 or 333 K under magnetic stirring of 2500 rpm. Sample analyses were performed on a GC-system with FID detector and a polar column (HP-5, L=30 m). Mass balances were accurate to within 5%.

Supplementary Figures and Tables

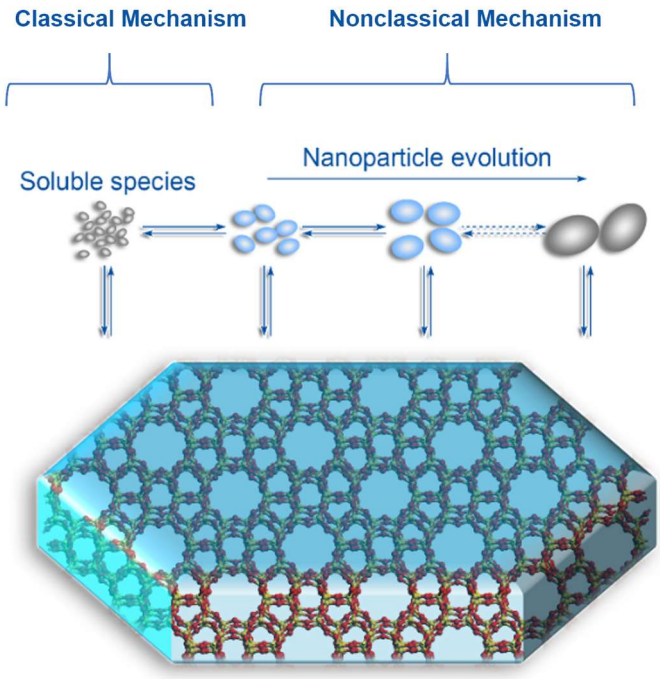

Figure S1. Putative crystallization pathways of silicalite-1 zeolite by monomer addition and the attachment of as-synthesized and evolved nanoparticles.[1, 2]

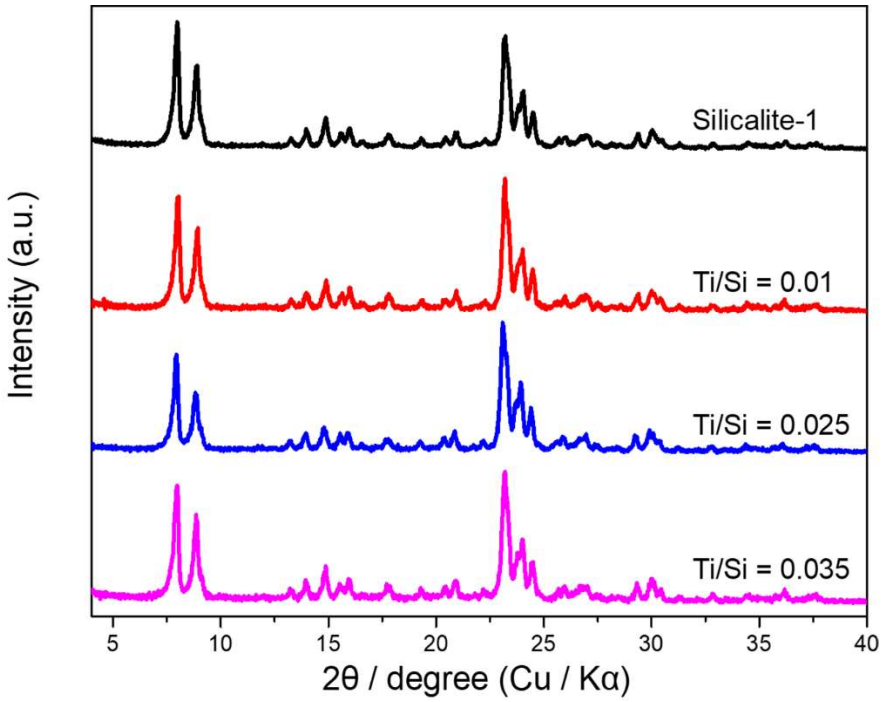

Figure S2. XRD patterns of Silicalite-1 and TS-1 zeolites with various Ti/Si = 0.01, 0.025, and 0.035.

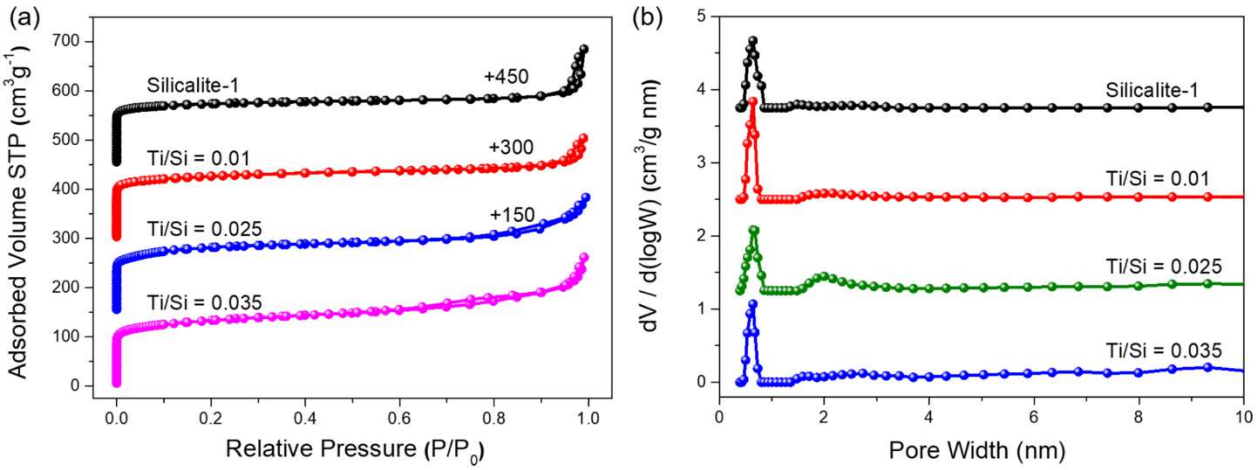

Figure S3. (a) N_2 adsorption-desorption isotherms and (b) pore size distributions of Silicalite-1 and TS-1 zeolites with Ti/Si = 0.01, 0.025, and 0.035.

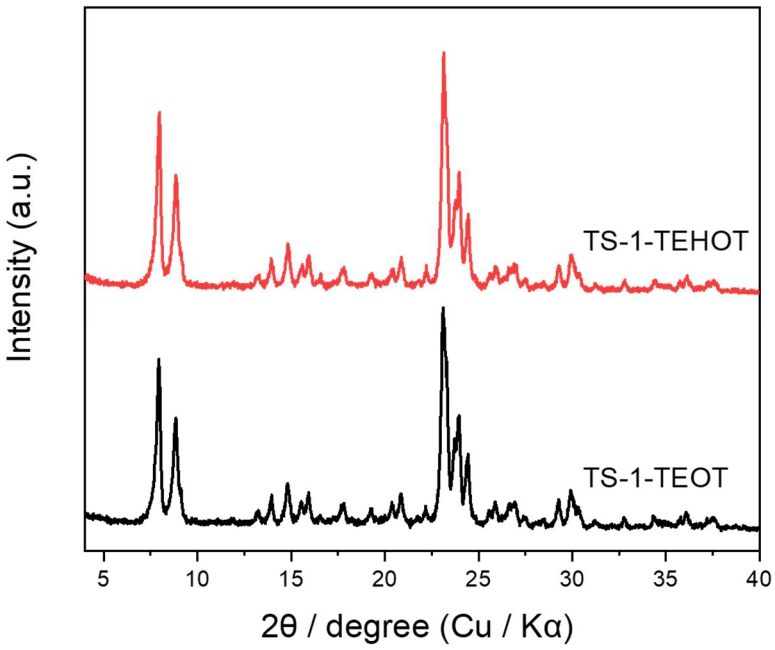

Figure S4. XRD patterns of TS-1-TEOT and TS-1-TEHOT.

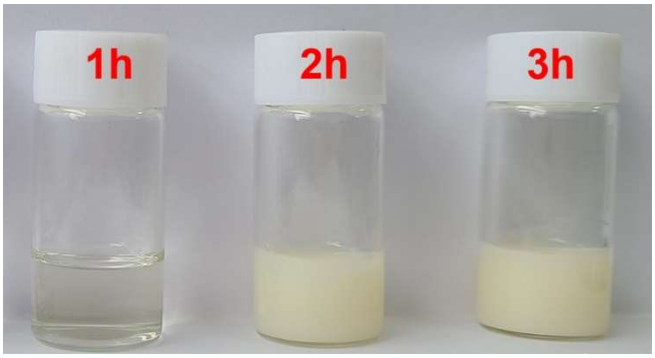

Figure S5. Photograph of TS-1-TEOT samples crystallized at 170 °C for different times.

Figure S6. Photograph of TS-1-TBOT (also named as TS-1-TBOT-10) samples crystallized at 170 °C for different times.

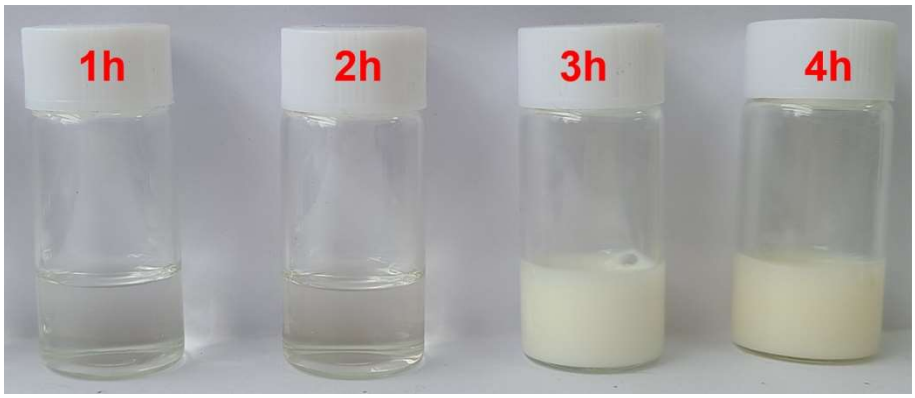

Figure S7. Photograph of TS-1-TEHOT samples crystallized at 170 °C for different times.

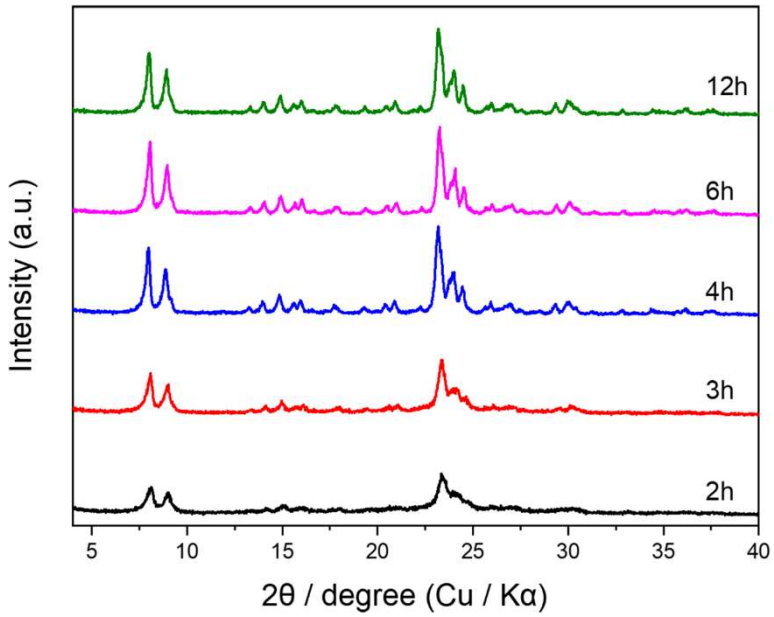

Figure S8. XRD patterns of TS-1-TEOT crystallized at 170 °C for different times.

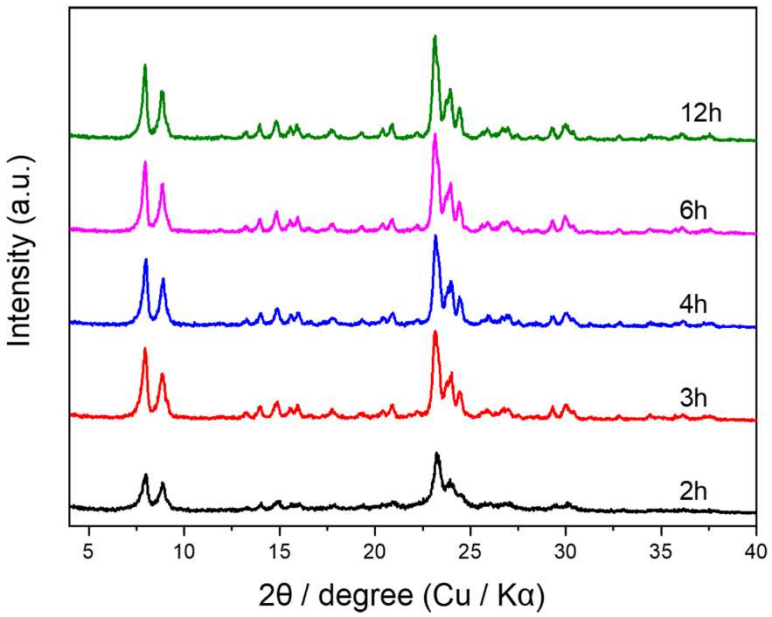

Figure S9. XRD patterns of TS-1-TBOT (also named as TS-1-TBOT-10) crystallized at 170 °C for different times.

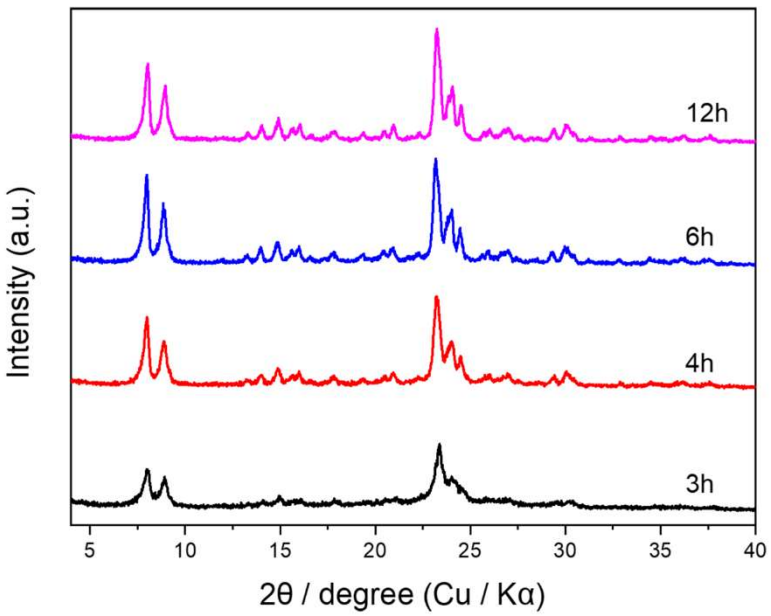

Figure S10. XRD patterns of TS-1-TEHOT crystallized at 170 °C for different times.

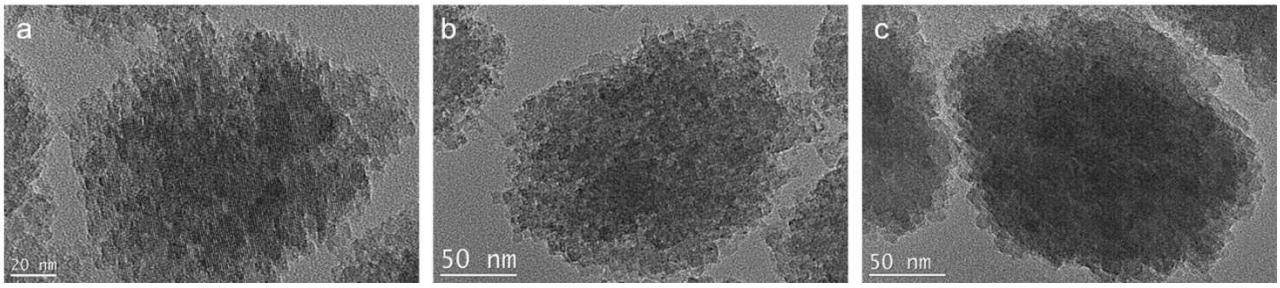

Figure S11. TEM images of (a) TS-1-TEOT-2h, (b) TS-1-TBOT-2h, and (c) TS-1-TEHOT-3h.

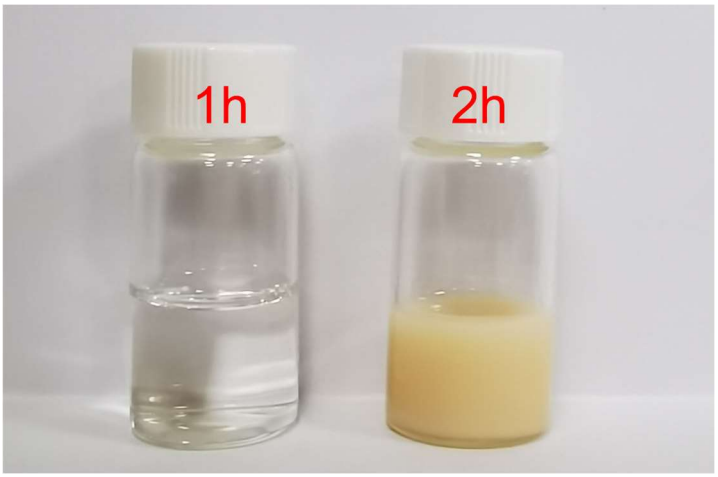

Figure S12. Photograph of TS-1-TEOT-iso-octanol samples crystallized at 170 °C for different times.

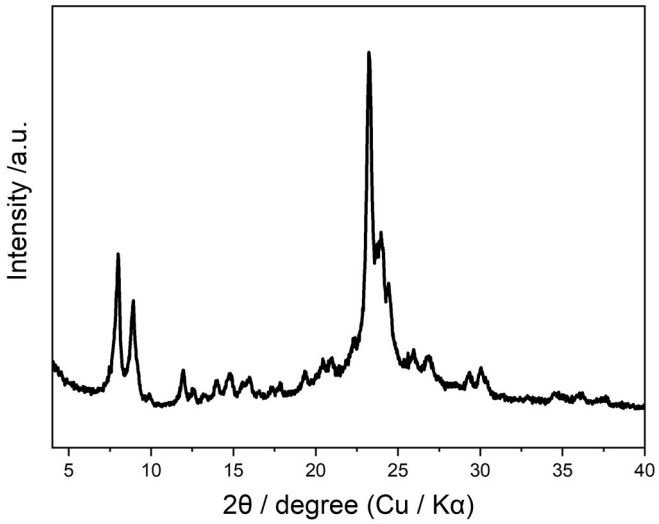

Figure S13. XRD pattern of TS-1-TEOT-iso-octanol crystallized at 170 °C for 2 h.

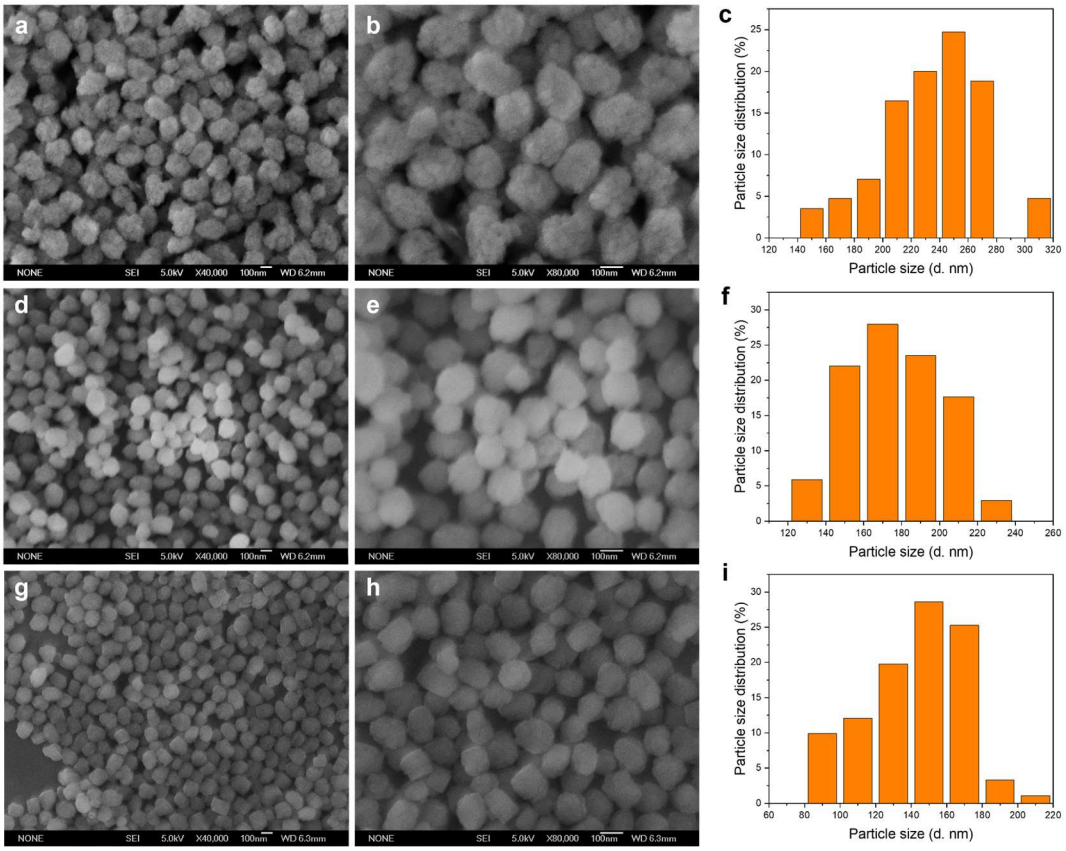

Figure S14. SEM images and the corresponding crystal particle distributions of the TS-1-TEOT (a-c), TS-1-TEOT-butanol (d-f), and TS-1-TEOT-iso-octanol (g-i). Above mentioned zeolites were prepared with the synthesis gel composition of 1.0 SiO_2: 0.025 TEOT: (0.1 butanol or iso-octanol): 0.2 TPAOH: 10 H_2O at 170 °C for 24 h.

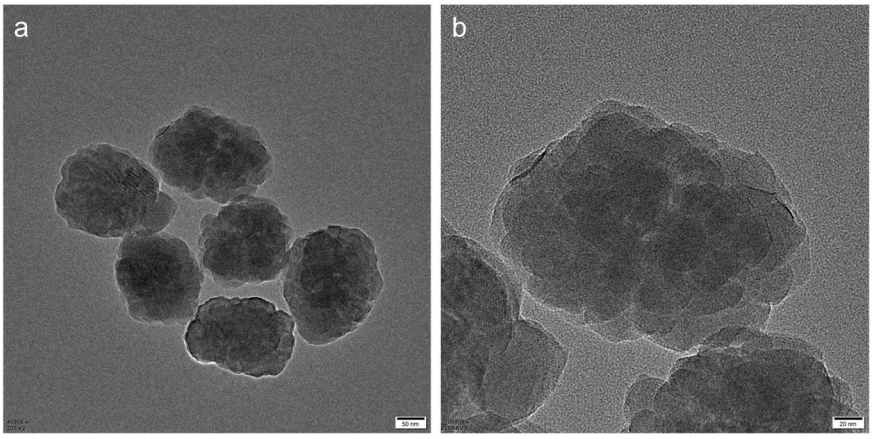

Figure S15. TEM images of TS-1-TEOT-iso-octanol crystallized at 170 °C for 24 h.

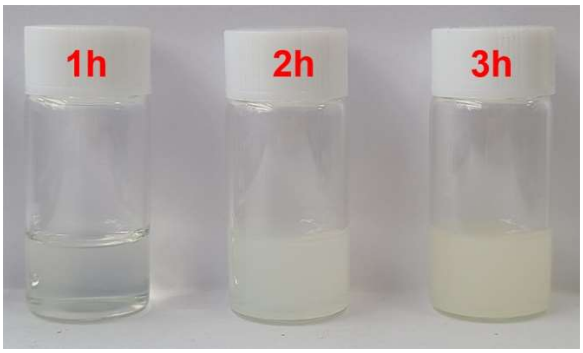

Figure S16. Photograph of TS-1-TBOT-20 samples crystallized at 170 °C for different times.

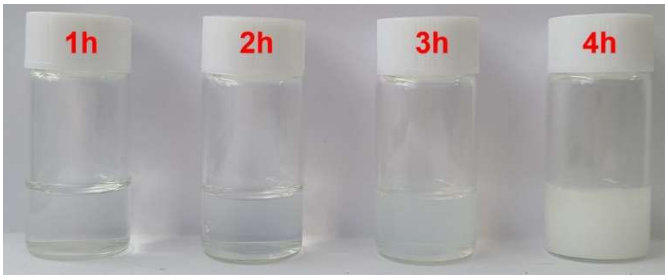

Figure S17. Photograph of TS-1-TBOT-40 samples crystallized at 170 °C for different times.

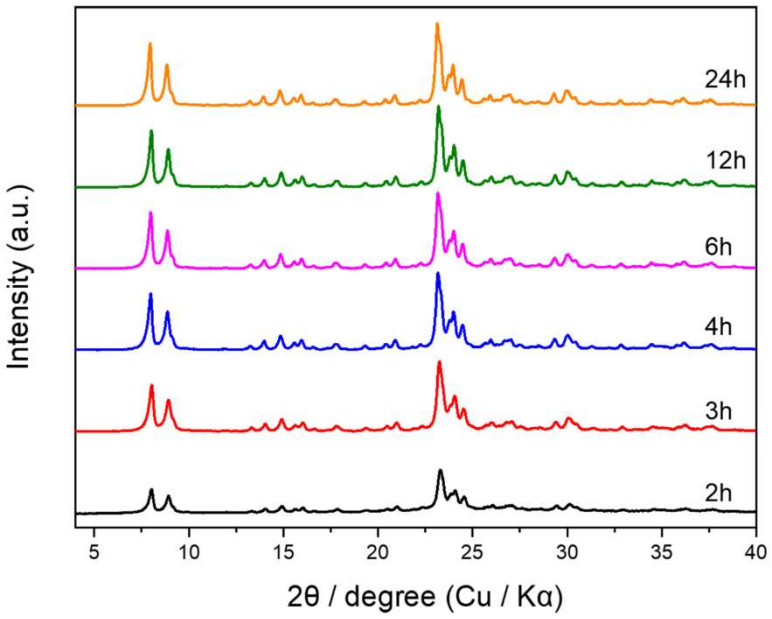

Figure S18. XRD patterns of TS-1-TBOT-20 crystallized at 170 °C for different times.

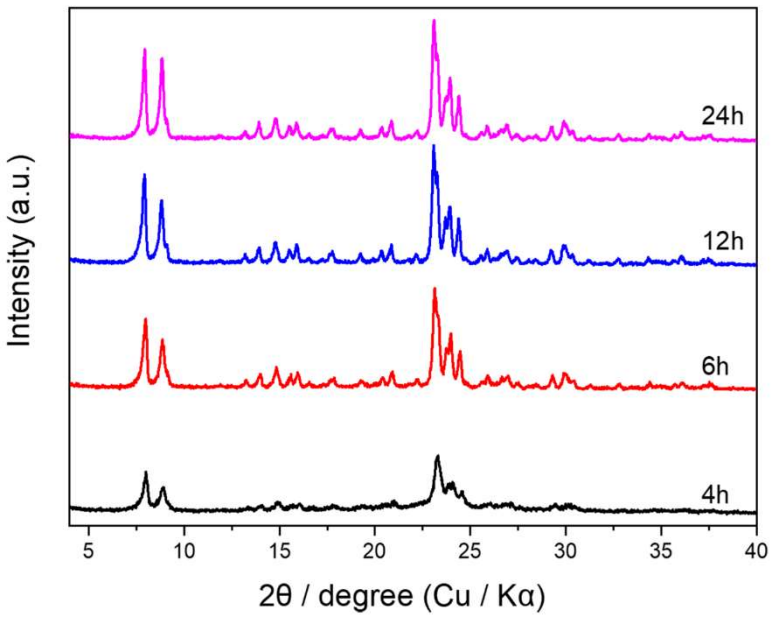

Figure S19. XRD patterns of TS-1-TBOT-40 crystallized at 170 °C for different times.

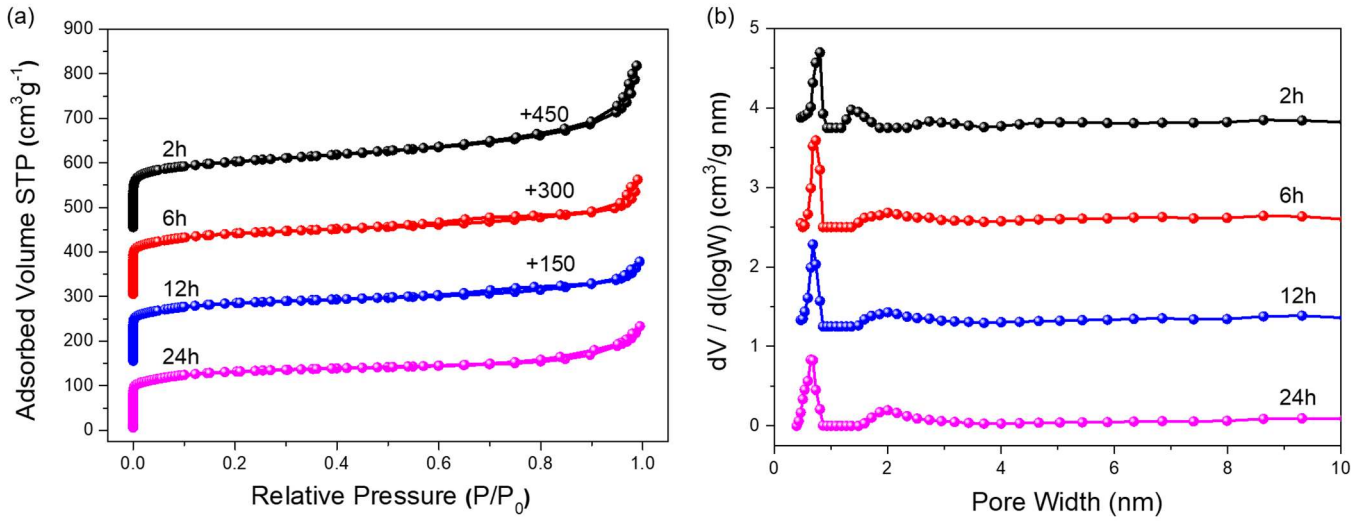

Figure S20. (a) N_2 adsorption-desorption isotherms and (b) pore size distributions of TS-1-TBOT samples crystallized for different times (TS-1-TBOT-2h, TS-1-TBOT-6h, TS-1-TBOT-12h, and TS-1-TBOT-24h (also named as TS-1-TBOT/TS-1-TBOT-10)).

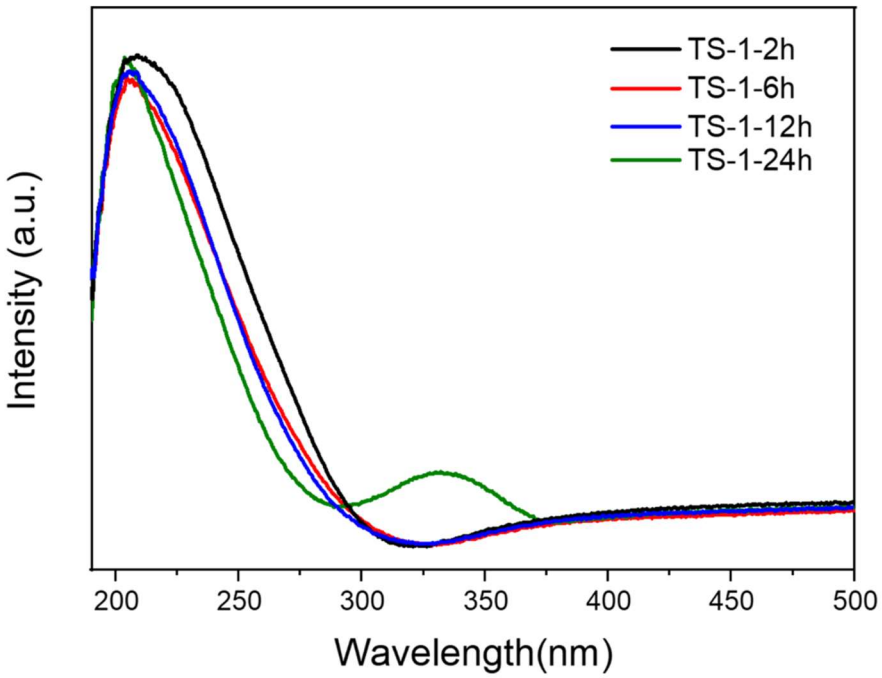

Figure S21. UV-vis spectra of TS-1-TBOT zeolite samples, crystallized for different times.

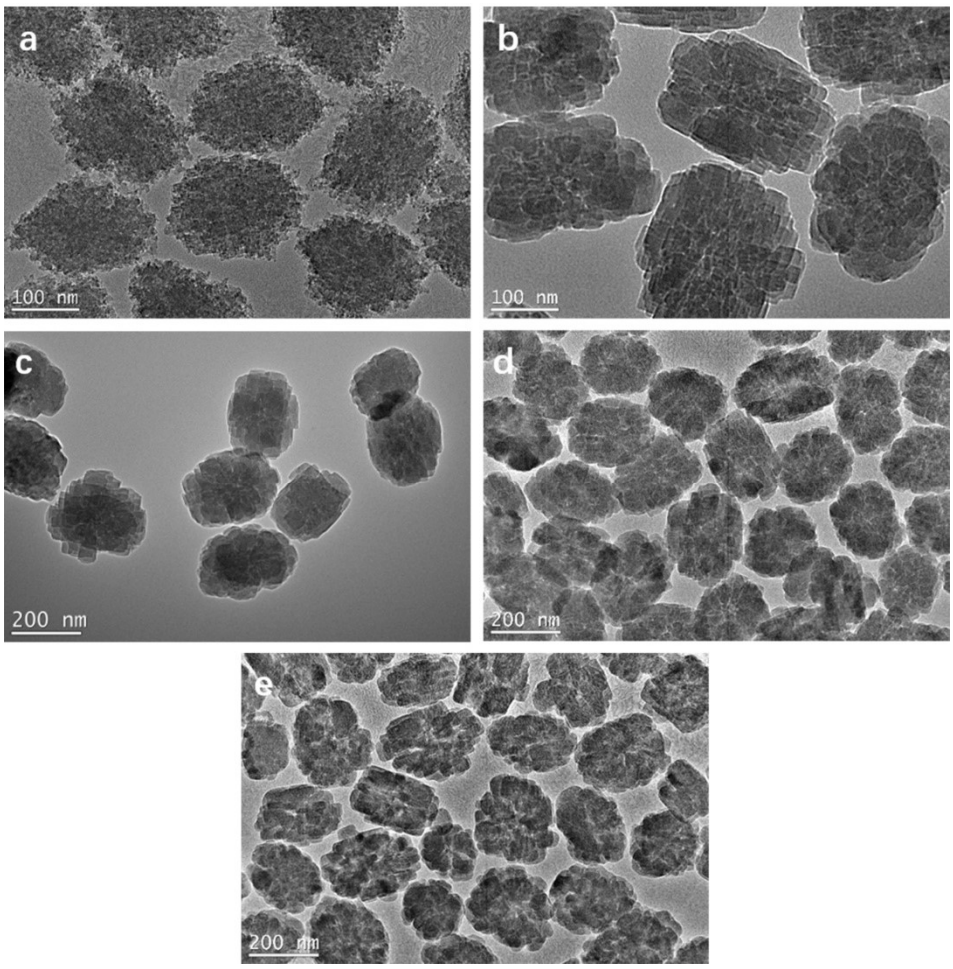

Figure S22. TEM images of TS-1-TBOT zeolites crystallized for different crystallization times. (a) 2 h, (b) 6 h, (c) 9 h, (d) 12 h, and (e) 24 h.

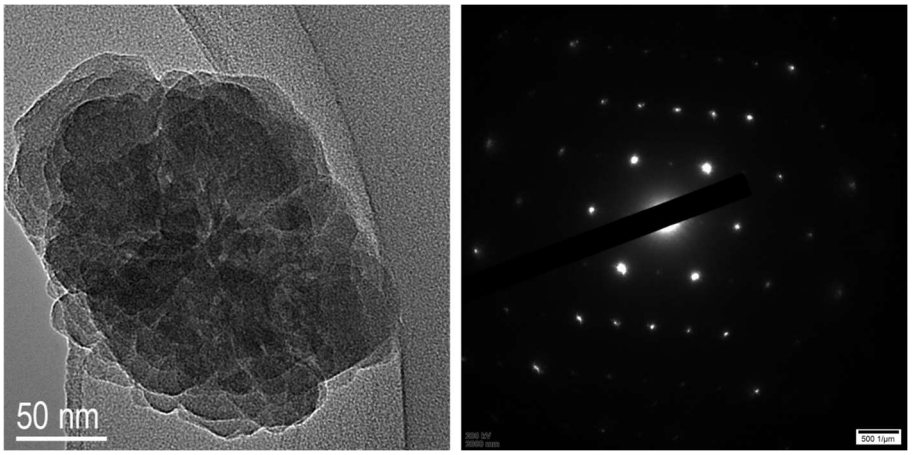

Figure S23. TEM image and the corresponding FFT pattern of TS-1-TBOT zeolites crystallized for 24 h.

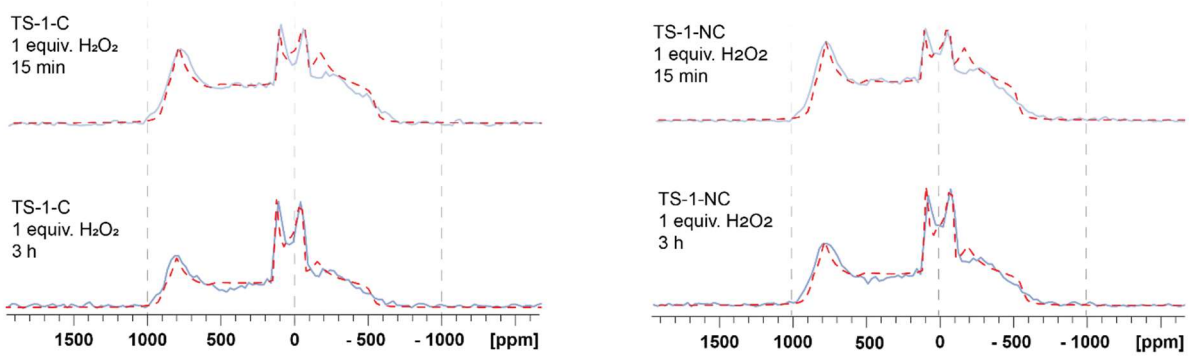

Figure S24. Reconstructed echo spectrum at given time points (15 min and 3 h) for TS-1-C and TS-1-NC (blue) and fit (red).

Note: An overlay of only the reconstructed echo spectra and the sum of the fitted components can be seen in Figure S24. The spectra are fully described by the two fitted components. A small error arises in the region around -150 ppm, which is due to the difficulty to determine all three Euler angles precisely through measurements at one single field, it has however no significant impact on the quantification described herein.

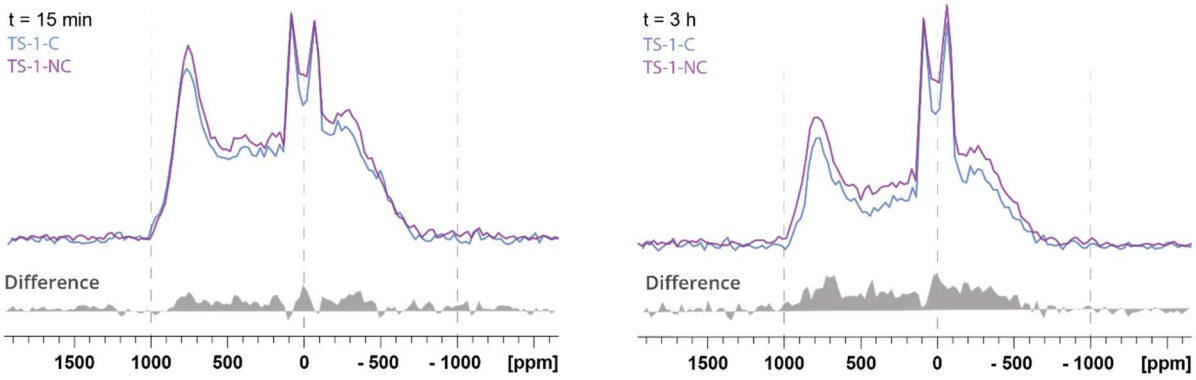

Figure S25. Overlay of reconstructed echo spectra of TS-1-C and TS-1-NC at given time points (15 min and 3 h).

Note: Reconstructed echo spectra of TS-1-C and TS-1-NC at the given times are shown in Figure S25. As stated, the peroxo on TS-1-NC is slightly more stable / decomposes slightly slower than for TS-1-C. In numerical values, this difference is best given by the ratio of the integrals of the two species (normalized to 100 in the manuscript). The difference spectra (normalized by the maximum intensity of the water signal) show clear differences above the noise level and also an increasing difference with time, further demonstrating the sensitivity of our approach.

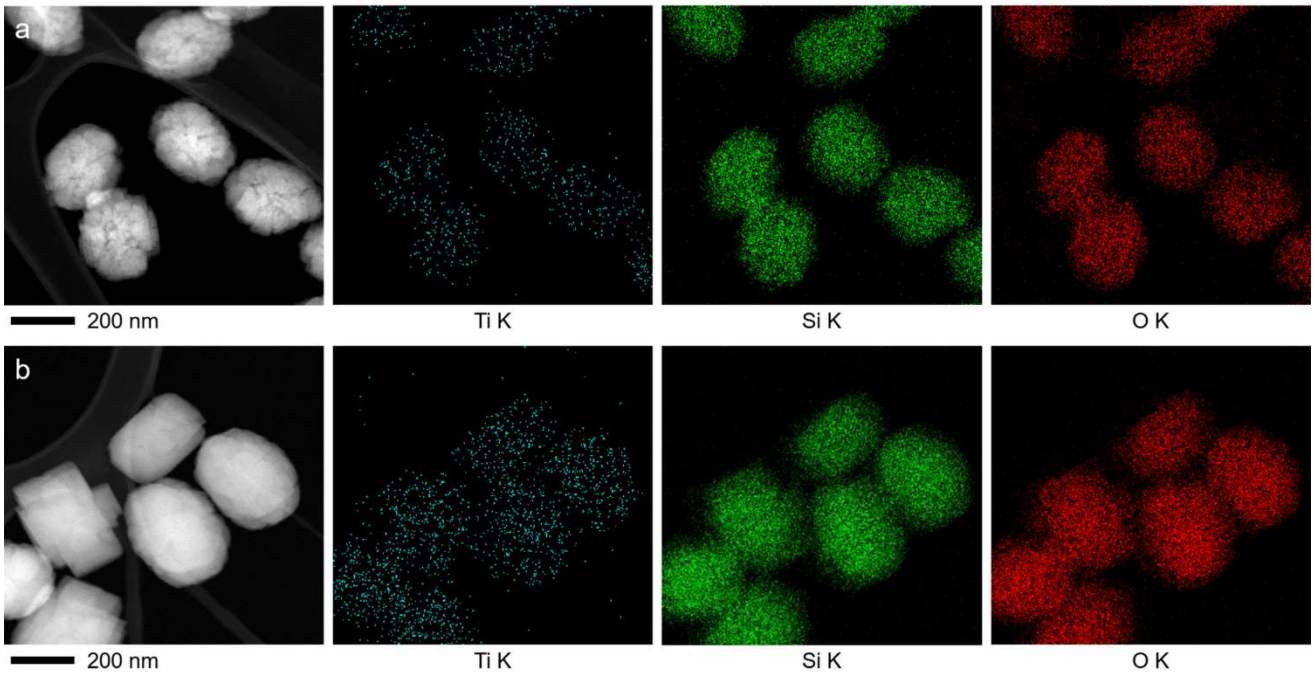

Figure S26. Bright field TEM images and elemental mappings for Si, O and Ti elements of (a) TS-1-NC and (b) TS-1-C.

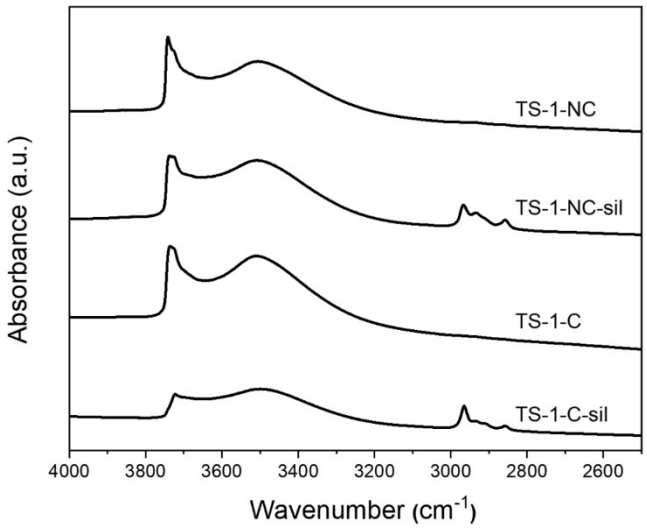

Figure S27. IR spectra of TS-1-NC, TS-1-NC-sil, TS-1-C, and TS-1-C-sil.

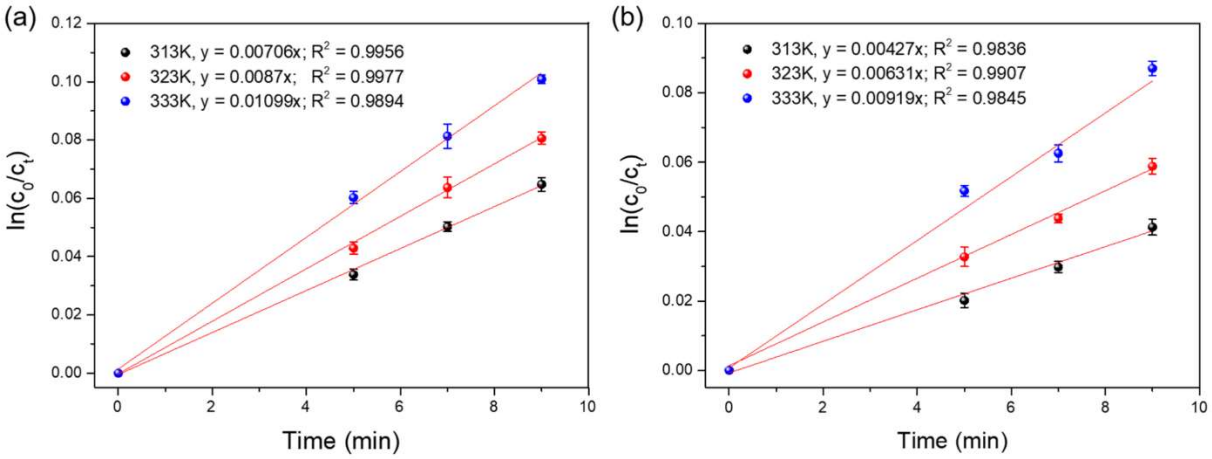

Figure S28. Pseudo-first-order rate constants of (a) TS-1-NC and (b) TS-1-C for the epoxidation of 1-hexene at different temperatures; reaction conditions: cat., 33 mg; 1-hexene, 16 mmol; H_2O_2 (35 wt%), 4 mmol; methanol, 12 g, and 3 bar of N_2.

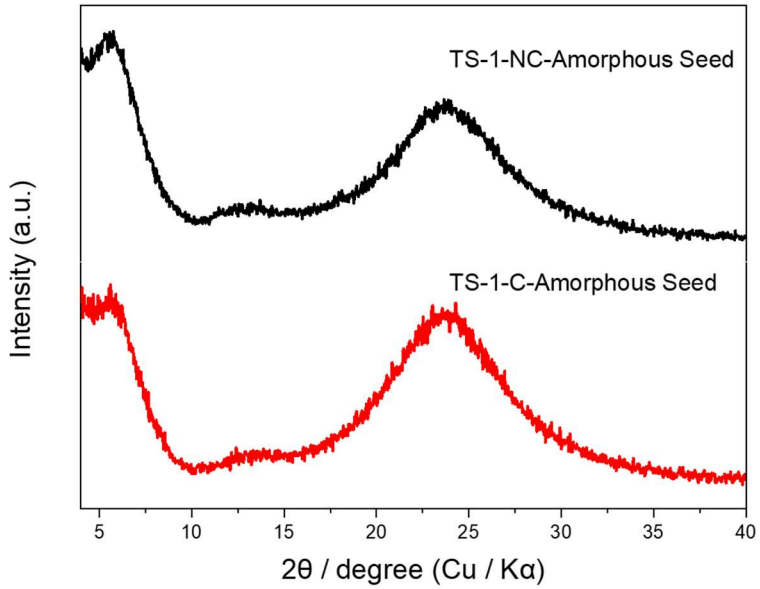

Figure S29. XRD patterns of the titanosilicate precursor seeds.

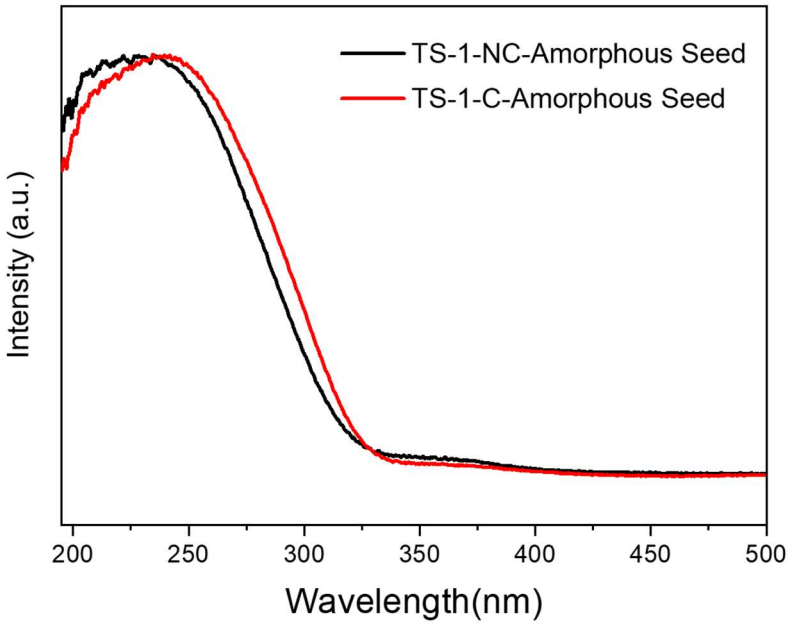

Figure S30. UV-vis spectra of the titanosilicate precursor seeds.

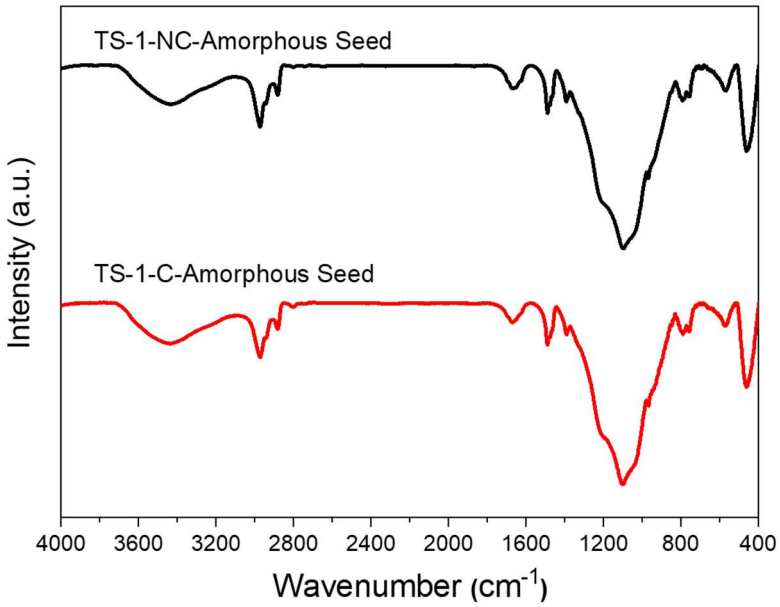

Figure S31. FT-IR spectra of the titanosilicate precursor seeds.

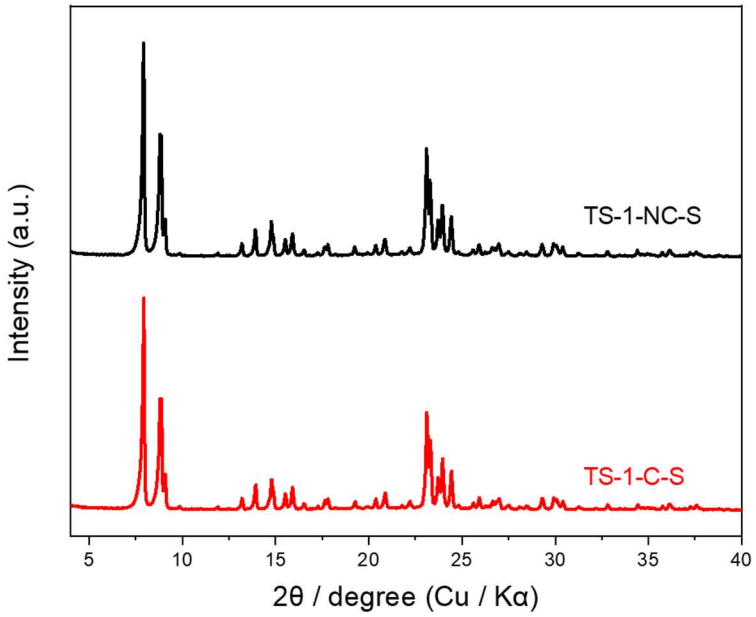

Figure S32. XRD patterns of the TS-1 zeolite samples prepared by using titanosilicate precursor seeds.

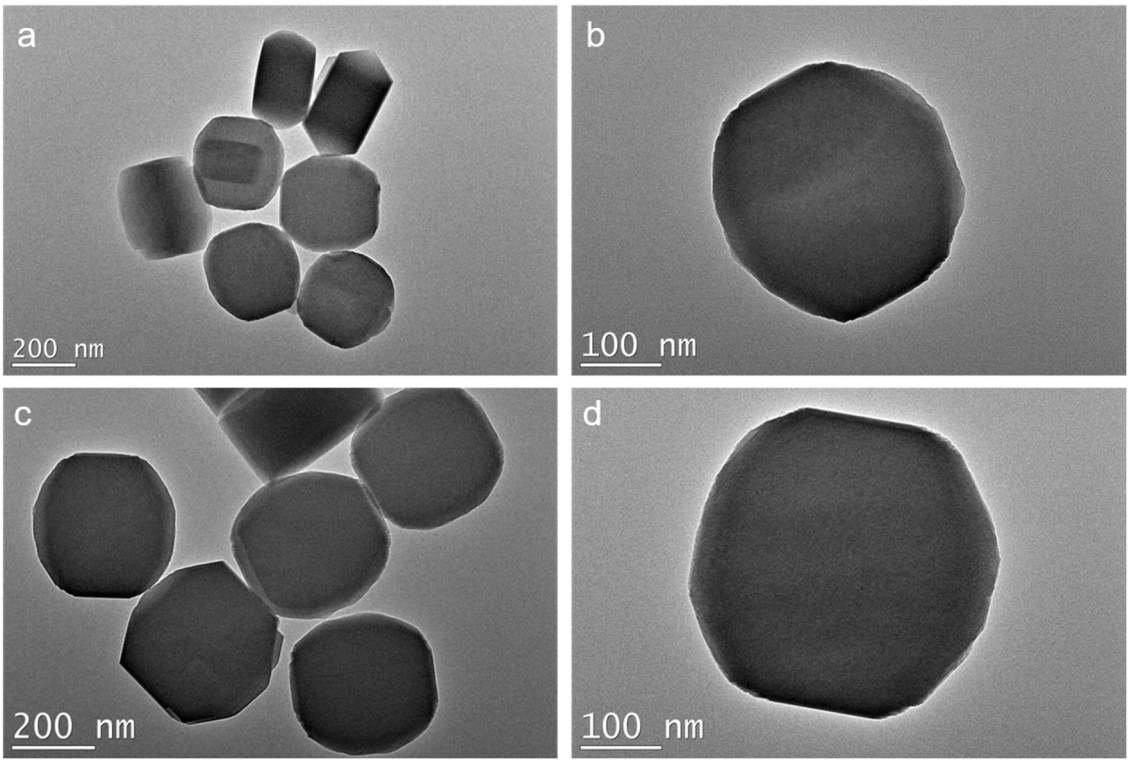

Figure S33. TEM images of the (a, b) TS-1-NC-S and (c, d) TS-1-C-S samples prepared by using titanosilicate precursor seeds.

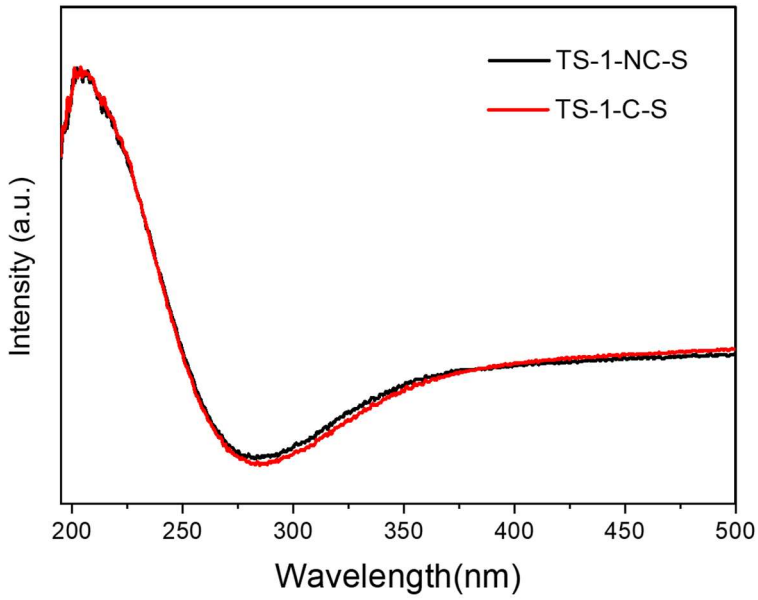

Figure S34. UV-vis spectra of the TS-1 zeolite samples prepared by using titanosilicate precursor seeds.

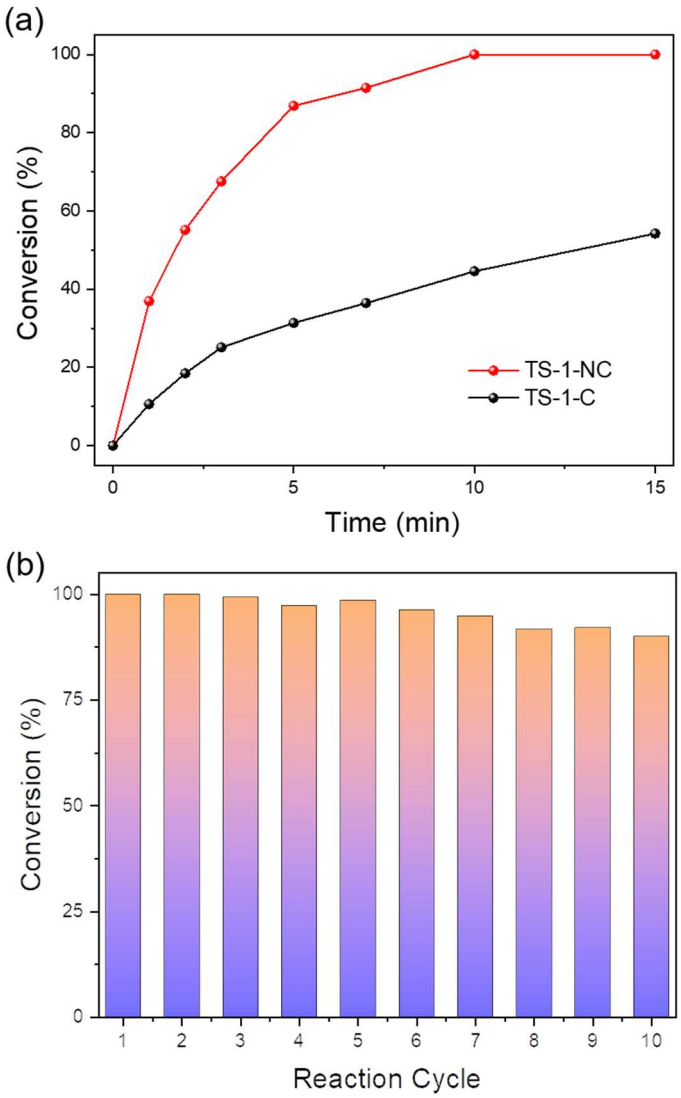

Figure S35. (a) Time-course variation of 4,6-DMDBT conversion over the TS-1-NC and TS-1-C catalysts at 343 K. (b) Recycle tests in the oxidation of 4,6-DMDBT over TS-1-NC zeolite catalyst. Reaction conditions: 10 mL of model fuels with S content of 500 ppm, n(sulphide) / n(TBHP) = 0.5, 30 mg of catalyst.

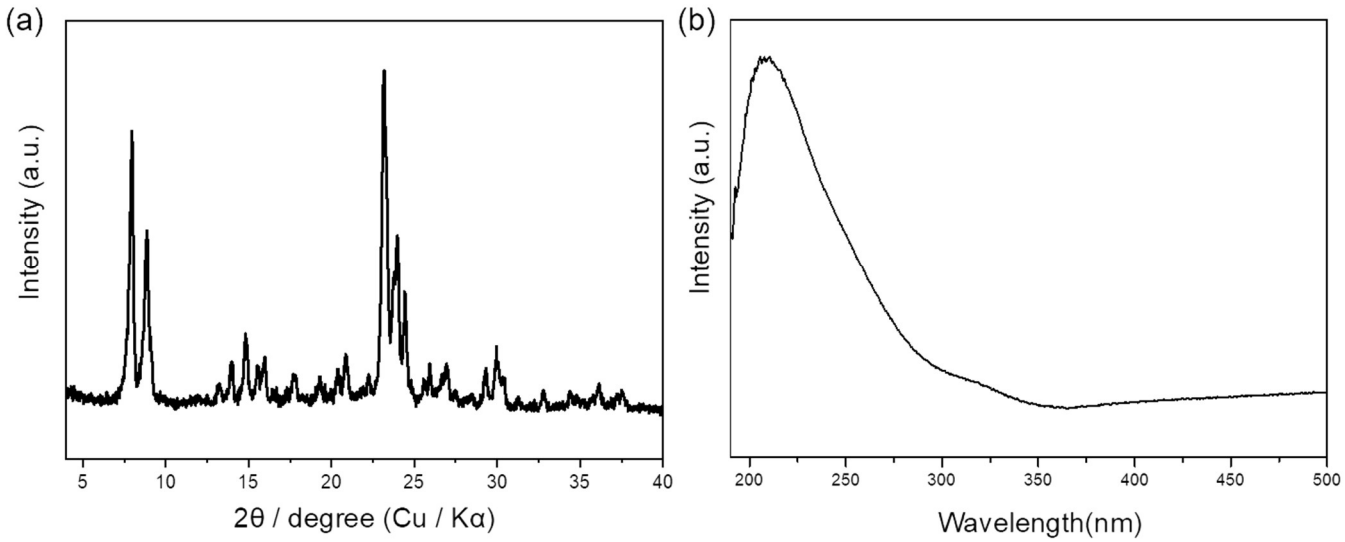

Figure S36. (a) XRD pattern and (b) UV-vis spectrum of TS-1-NC zeolite catalyst after 10 cycles of reaction.

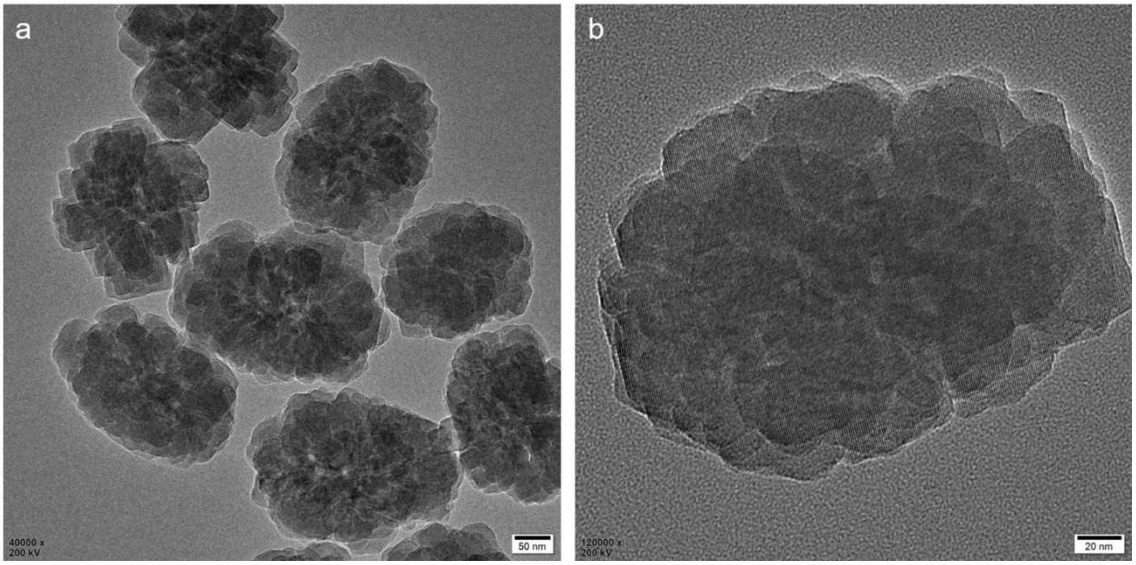

Figure S37. TEM images of TS-1-NC zeolite catalyst after 10 cycles of reaction.

Table S1. Textural porosities of the prepared zeolite samples.

Sample	S_{BET}[a] (m^2/g)	S_{micro}[b] (m^2/g)	S_{ext}[b] (m^2/g)	V_{total}[c] (cm^3/g)	V_{micro}[b] (cm^3/g)	V_{meso}[d] (cm^3/g)
Silicalite-1	483	346	137	0.36	0.13	0.23
TS-1 (Ti/Si=0.01)	480	301	179	0.32	0.12	0.20
TS-1 (Ti/Si=0.025) (TS-1-TBOT-10; TS-1-TBOT-24h)	493	300	193	0.35	0.12	0.23
TS-1 (Ti/Si=0.035)	494	291	203	0.41	0.12	0.29
TS-1-TBOT-20	475	299	176	0.25	0.12	0.13
TS-1-TBOT-40	464	331	133	0.21	0.13	0.08
TS-1-TBOT-2h	560	240	320	0.57	0.10	0.47
TS-1-TBOT-6h	525	288	237	0.41	0.12	0.29
TS-1-TBOT-12h (TS-1-NC)	502	294	208	0.35	0.12	0.23
TS-1-C	457	296	161	0.27	0.12	0.15

[a]Specific surface area calculated from the nitrogen adsorption isotherm using the BET method. [b]S_{micro} (micropore area), S_{ext} (external surface area), and V_{micro} (micropore volume) calculated using the t-plot method. [c]Total pore volume at $P/P_0 = 0.995$. [d]$V_{meso} = V_{total} - V_{micro}$.

Table S2. Oxidation of 1-hexene over TS-1-NC.[a]

Time (min)	Conv.	H_2O_2		Select.(%)		
	Max. (%)	Conv. (%)	Effic. (%)	epoxide	Monomethyl glycol ether	Glycol
30	74.2	91.6	81.0	83.8	13.2	2.3
60	74.3	91.8	80.9	80.6	17.5	1.1
120	75.3	92.2	81.7	80.4	18.1	1.2
180	76.1	92.4	82.4	70.2	25.3	3.4
300	76.9	93.7	82.0	69.5	25.7	4.0

[a]Reaction conditions: cat., 100 mg; 1-hexene, 16 mmol; H_2O_2 (35 wt%), 4 mmol; methanol, 12 g; temp., 333 K, 3 bar of N_2.

Table S3. Oxidation of 1-hexene over TS-1-C.[a]

Time (min)	Conv.	H_2O_2		Select.(%)		
	Max. (%)	Conv. (%)	Effic. (%)	epoxide	Monomethyl glycol ether	Glycol
30	48.7	75.2	64.8	84.6	15.0	0.0
60	59.9	89.7	66.7	78.8	19.4	1.3
120	69.0	90.4	76.3	74.9	22.2	2.5
180	70.1	91.7	76.4	72.0	23.8	3.2
300	73.7	92.3	79.9	70.1	24.1	4.7

[a]Reaction conditions: cat., 100 mg; 1-hexene, 16 mmol; H_2O_2 (35 wt%), 4 mmol; methanol, 12 g; temp., 333 K, 3 bar of N_2.

Table S4. Oxidation of 1-hexene over TS-1-NC.[a]

Time (min)	Conv.	H_2O_2		Select.(%)		
	Max. (%)	Conv. (%)	Effic. (%)	Epoxide	Monomethyl glycol ether	Glycol
30	39.4	52.4	75.3	93.9	5.3	0.0
60	45.9	60.2	76.1	93.8	5.5	0.0
120	50.0	67.3	74.3	92.8	6.1	0.0
180	56.9	72.0	79.1	92.2	6.9	0.0

[a]Reaction conditions: cat., 33 mg; 1-hexene, 16 mmol; H_2O_2 (35 wt%), 4 mmol; methanol, 12 g; temp., 323 K, 3 bar of N_2.

Table S5. Oxidation of 1-hexene over TS-1-C.[a]

Time (min)	Conv.	H_2O_2		Select.(%)		
	Max. (%)	Conv. (%)	Effic. (%)	Epoxide	Monomethyl glycol ether	Glycol
30	33.8	45.9	73.5	92.9	6.4	0.0
60	38.6	52.2	74.1	91.9	7.2	0.0
120	41.4	55.7	74.2	90.1	8.5	0.0
180	50.6	67.5	75.0	90.5	8.8	0.0

[a]Reaction conditions: cat., 33 mg; 1-hexene, 16 mmol; H_2O_2 (35 wt%), 4 mmol; methanol, 12 g; temp., 323 K, 3 bar of N_2.

Table S6. Oxidation of 1-hexene over TS-1-NC-sil.[a]

Time (min)	Conv.	H_2O_2		Select.(%)		
	Max. (%)	Conv. (%)	Effic. (%)	Epoxide	Monomethyl glycol ether	Glycol
30	73.6	79.7	92.4	87.3	12.2	0.0
60	73.7	88.1	83.6	84.5	15.1	0.0
120	75.1	89.0	84.3	81.6	17.4	0.0
180	75.8	90.6	83.7	78.4	19.6	1.1
300	77.1	90.8	84.9	74.8	22.7	1.4

[a]Reaction conditions: cat., 100 mg; 1-hexene, 16 mmol; H_2O_2 (35 wt%), 4 mmol; methanol, 12 g; temp., 333 K, 3 bar of N_2.

Table S7. Oxidation of 1-hexene over TS-1-C-sil.[a]

Time (min)	Conv.	H_2O_2		Select.(%)		
	Max. (%)	Conv. (%)	Effic. (%)	Epoxide	Monomethyl glycol ether	Glycol
30	48.1	59.8	80.5	82.2	17.3	0.0
60	54.0	69.5	77.8	78.3	21.2	0.0
120	58.8	78.1	75.3	74.7	23.0	1.3
180	62.2	80.3	77.5	71.6	24.7	2.4
300	63.5	85.4	74.3	69.9	25.8	2.9

[a]Reaction conditions: cat., 100 mg; 1-hexene, 16 mmol; H_2O_2 (35 wt%), 4 mmol; methanol, 12 g; temp., 333 K, 3 bar of N_2.

Table S8. Oxidation of 1-hexene over TS-1-NC-S.[a]

Time (min)	Conv.	H_2O_2		Select.(%)		
	Max. (%)	Conv. (%)	Effic. (%)	Epoxide	Monomethyl glycol ether	Glycol
60	7.1	9.2	77.9	>99	0.0	0.0
120	8.7	10.8	80.4	>99	0.0	0.0
180	10.5	13.9	75.0	>99	0.0	0.0
300	14.7	20.1	72.9	>99	0.0	0.0

[a]Reaction conditions: cat., 100 mg; 1-hexene, 16 mmol; H_2O_2 (35 wt%), 4 mmol; methanol, 12 g; temp., 333 K, 3 bar of N_2.

Table S9. Oxidation of 1-hexene over TS-1-C-S.[a]

Time (min)	Conv.	H_2O_2		Select.(%)		
	Max. (%)	Conv. (%)	Effic. (%)	Epoxide	Monomethyl glycol ether	Glycol
60	6.3	10.3	60.8	>99	0.0	0.0
120	6.8	10.5	65.0	>99	0.0	0.0
180	8.4	12.9	65.1	>99	0.0	0.0
300	11.6	19.7	58.9	>99	0.0	0.0

[a]Reaction conditions: cat., 100 mg; 1-hexene, 16 mmol; H_2O_2 (35 wt%), 4 mmol; methanol, 12 g; temp., 333 K, 3 bar of N_2.

Table S10. Oxidation of 2-methyl-2-butene over TS-1-NC.[a]

Time (min)	Conv.	Select.(%)	
	Max. (%)	Epoxide	Others
30	11.7	51.1	48.9
60	13.4	51.1	48.9
120	18.5	34.2	65.8
180	22.4	26.7	73.3
300	29.8	18.5	81.5

[a]Reaction conditions: cat., 100 mg; 2-methyl-2-butene, 16 mmol; H_2O_2 (35 wt%), 4 mmol; acetonitrile, 12 g; temp., 323 K, 3 bar of N_2.

Table S11. Oxidation of 2-methyl-2-butene over TS-1-C.[a]

Time (min)	Conv.	Select.(%)	
	Max. (%)	Epoxide	Others
30	4.2	75.2	24.8
60	6.6	58.6	41.4
120	8.9	46.7	53.3
180	10.7	40.9	59.1
300	13.3	31.1	68.9

[a]Reaction conditions: cat., 100 mg; 2-methyl-2-butene, 16 mmol; H_2O_2 (35 wt%), 4 mmol; acetonitrile, 12 g; temp., 323 K, 3 bar of N_2.

Table S12. Oxidation of cyclohexene over TS-1-NC.[a]

Time (min)	Conv.	Select.(%)	
	Max. (%)	Epoxide	Others
30	18.4	41.8	58.2
60	23.9	43.0	57.0
120	32.9	43.5	56.5
180	36.3	45.1	54.9
300	46.1	44.1	55.9

[a]Reaction conditions: cat., 100 mg; cyclohexene, 16 mmol; H_2O_2 (35 wt%), 4 mmol; acetonitrile, 12 g; temp., 323 K, 3 bar of N_2.

Table S13. Oxidation of cyclohexene over TS-1-C.[a]

Time (min)	Conv.	Select.(%)	
	Max. (%)	Epoxide	Others
30	4.7	51.8	48.2
60	11.5	45.5	54.5
120	14.5	41.9	58.1
180	16.2	38.5	61.5
300	23.1	34.0	66.0

[a]Reaction conditions: cat., 100 mg; cyclohexene, 16 mmol; H_2O_2 (35 wt%), 4 mmol; acetonitrile, 12 g; temp., 323 K, 3 bar of N_2.

References

1. Davis, T. M.; Drews, T. O.; Ramanan, H.; He, C.; Dong, J.; Schnablegger, H.; Katsoulakis, M. A.; Kokkoli, E.; McCormick, A. V.; Penn, R. L.; Tsapatsis, M., Mechanistic Principles of Nanoparticle Evolution to Zeolite Crystals. *Nature Materials* **2006,** *5* (5), 400-408.

2. Lupulescu, A. I.; Rimer, J. D., In Situ Imaging of Silicalite-1 Surface Growth Reveals the Mechanism of Crystallization. *Science* **2014,** *344* (6185), 729-732.